SUPPORTING INFORMATION

Structural Characterisation of a Model Gram-negative Bacterial Surface Using Lipopolysaccharides from Rough Strains of *Escherichia coli*

Anton P. Le Brun, Luke A. Clifton, Candice E. Halbert, Binhua Lin, Mati Meron, Peter J. Holden, Jeremy H. Lakey and Stephen A. Holt

SUPPORTING EXPERIMENTAL SECTION

Detailed description of fermentation and deuterated RcLPS extraction

E. coli J5 (Rc mutant, ATCC # 43745) from a glycerol stock was streaked onto an LB-agar plate. The *E. coli* cells were adapted to D_2O in a step-wise manner as described by Chen *et al.*[1] A colony was picked and grown in 10 mL of LB media at 37 °C with shaking until confluent. The culture from the LB media was then used to inoculate 10 mL of ModC1 media made with H_2O (40 g L^{-1} glycerol, 4.16 g L^{-1} Na_2HPO_4, 2.58 g L^{-1} NH_4Cl, 2.54 g L^{-1} KH_2PO_4, 1.94 g L^{-1} K_2SO_4, 0.33 g L^{-1} $MgSO_4$, 0.1 g L^{-1} sodium citrate, 4.8 mg L^{-1} Thiamine-HCl, 0.91 mg L^{-1} $FeCl_2$, 0.49 mg L^{-1} $CuSO_4$, 0.44 mg L^{-1} $MnCl_2$ and 0.41 mg L^{-1} $ZnCl_2$) which was grow at 37 °C with shaking until confluent. The *E. coli* J5 cells were adapted to D_2O by transferring confluent cultures to fresh ModC1 media with increasing amounts of D_2O starting at 50 % D_2O, then 75 % D_2O and finally 100 % D_2O. The D_2O adapted cultures were then used to inoculate a fermenter, with 1 L 100 % D_2O ModC1 media with 40 g L^{-1} ^{1}H-glycerol as the carbon source, to a starting OD_{600} of 0.1. Cells were cultured at 37 ˚C with the stirrer rate set to maintain a minimum dissolved oxygen tension of 30% using an air flow of 0.5 L min^{-1}. The pH was controlled by the addition of ammonium hydroxide with a set point of pH 7.0. When the glycerol carbon source was exhausted (OD_{600} = 20.8) the cells

were harvested by centrifugation (36 g of wet cell mass). The wet cell mass was washed with water and then ethanol and freeze dried.

Using the method originally from Galanos *et al*.[2] dried cells were gently homogenized in phenol/chloroform/petroleum spirit (2:5:8 v:v:v) using 10 mL for every gram of dry cells. The homogenate was then centrifuged in glass centrifuge tubes at 4000 $\times g$ for 15 minutes. The supernatant was kept and the pellet re-homogenized in the organic mixture. A total of three extractions were carried out. The supernatant from each extraction was pooled and filtered under vacuum using a coarse filter. The chloroform and petroleum spirit were removed by rotary evaporation. 5 mL of diethyl ether/acetone (1:1 v:v) was added drop wise until a white precipitate formed in the phenolic solution. The solution was left overnight to allow for complete precipitation of the RcLPS. The RcLPS was isolated by centrifugation at 4000 $\times g$ for 30 min in glass tubes. The supernatant was discarded and the pellet washed with 80 % phenol to remove protein contaminates and then with diethyl ether to remove excess phenol with centrifugation at 4000 $\times g$ for 30 min between each wash. The pellet was then dissolved in ultrapure water by sonication at 45 ˚C. To isolate the pure RcLPS, high speed centrifugation at 100 000 $\times g$ for 4 h was carried out and the resulting pellet contained pure RcLPS.

LPS vesicles were created by dissolving lyophilized LPS in 20 mM sodium phosphate pH 7.0 and warming to 45 °C for 1 hour. The LPS solution was then sonicated in a sonic bath for one hour at 45 °C. The formation of vesicles was verified by dynamic light scattering using a Watt DynaPro Titan DLS instrument (Santa Barbra, CA, USA).

Analysis of neutron reflectivity data

Data was analyzed using the MOTOFIT reflectivity analysis software [3] which uses the optical matrix method.[4] The monolayer can be divided into a series of sub-layers and each sub-layer is described by its thickness (in units Å), neutron scattering length density (nSLD, in units $Å^{-2}$) and Gaussian interfacial roughness (in units Å). A least squares fitting routine selects the best fit by minimizing χ^2 values by varying the parameters of each layer. χ^2 was minimized by a genetic algorithm to reduce the likelihood of falling into local χ^2 minima. The model fitting of the reflectivity profiles yields information on the neutron scattering length density (nSLD) profile normal to the surface. The nSLD can be considered to be the neutron reflective index and is a function of the chemical composition of each material according to

$$nSLD = N_A \sum_i \frac{p_i}{A_i} b_i$$

where N_A is Avogadro's number, p_i the mass density, A_i the atomic mass and bi the nuclear scattering length of component i. In neutron scattering the nuclear scattering length varies from element to element *and* from isotope to isotope. In this case the difference in scattering length between hydrogen (^1H) (b_H = -3.74 $\times 10^{-5}$ Å) and its isotope deuterium (^2H) (b_D = +6.67 $\times 10^{-5}$ Å) is particularly useful. By deuteration of components and choosing the correct isotopic solvent contrasts, different components of the system can be highlighted or made 'invisible' to the neutrons. The monolayer system was divided into discrete layers and the nSLD of the layer is the sum of the nSLD of all components in the layer, i.e.

$$nSLD_{layer} = (\emptyset_{LPS} \times nSLD_{LPS}) + (\emptyset_{solvent} \times nSLD_{solvent})$$

where φ is the volume fraction of the component which can be calculated by comparing fitted values with the theoretical values in Supplementary Table S1. Each contrast is fitted simultaneously and the physical structure of the monolayer is

assumed to be stable when isotopic solvent contrasts are changed. Therefore, when changing contrasts, the thickness and roughness are kept constant and with only the nSLD allowed to vary.

Estimates of parameter uncertainties were obtained through using a Monte Carlo resampling procedure[5,6] on the best data fits obtained using MOTOFIT. The parameter ranges obtained from the best fit are used in the resampling procedure where 1000 separate datasets are 'synthesized' from the original dataset by adding Gaussian noise, weighted by the counting statistics of the real data, to each data point. These synthesized datasets are fitted individually. The fits to the synthetic data were analyzed by histogramming the fitted values. The distribution of each parameter was statistically analyzed with the parameter value taken as the midpoint of the 95 % confidence interval and its uncertainty from the standard deviation of the distribution.

Analysis of GIXD data

Grazing incidence X-ray diffraction (GIXD) is performed with the x-ray beam at constant incidence angle with the surface, α_i, which is slightly below the critical angle, α_c, of the air-water interface.[7] The scattered intensity was measured in two dimensions as a function of the vertical scattering angle, α_f, where the angle between the incident and diffracted beam is $2\theta_{xy}$. By scanning $2\theta_{xy}$, the horizontal scattering vector (Q_{xy}) and the vertical scattering vector (Q_z) can be determined and are given by

$$Q_{xy} = \left(\frac{4\pi}{\lambda}\right)\sin\left(\frac{2\theta_{xy}}{2}\right)$$

$$Q_z = \left(\frac{2\pi}{\lambda}\right)\sin(\alpha_f)$$

The GIXD data was reduced so that three plots are produced. The first is a contour plot of intensity as a function of Q_{xy} and Q_z. By integrating the contour plot along Q_z yields the second plot which is a GIXD pattern of intensity *vs.* Q_{xy}. The GIXD patterns were then fitted for background and a Gaussian function fitted to each peak for information on peak position, relative intensity and full-width half maximum. The third plot is where the data is integrated along Q_{xy} to yield intensity *vs.* Q_z plots which provide profiles of the Bragg rods. The Q_{xy} positions of the in-plane Bragg rods correspond to repeat distances, d_{hk} (= $2\pi/Q_{xy}$), and can be indexed with Miller indices (h and k). Once the Miller indices have been allocated to each peak the 2D unit cell parameters (a, b, γ) can be calculated from the Gaussian peak position of each peak. In GIXD only the ordered 2D crystalline alkyl chains of the LPS contribute to the diffraction pattern. Therefore the chain-like cylindrical molecules can only pack as either a hexagonal (a = b, γ = 120˚), a distorted (rectangular) hexagonal (a ≠ b, γ = 90˚) or an oblique hexagonal (a ≠ b, γ ≠ 90˚).[8,9] The d_{hk}-spacing of an oblique hexagonal corresponds to

$$d = \left[\frac{h^2}{a^2} + \frac{k^2}{b^2} - 2\left(\frac{hk}{ab}\right)\cos\gamma\right]^{-1/2} \sin\gamma$$

from which the unit cell parameters can be extracted. The area of the unit cell, A_{cell} = a b sinγ is used to calculate the cross-sectional area per alkyl chain, A_o,

$$A_0 = A_{cell}\cos(t)$$

here t is the tilt angle. The tilt angle is derived from the out-of-plane peak [10] and is given by:

$$\tan(t) = \frac{Q_z}{Q_{xy}}$$

The full-width at half maximum (FWHM) of the fitted peaks that have been corrected for instrument resolution, yields information on the crystalline domain lengths, L_{xy}, of the monolayer by using the Scherrer formula:[7,8]

$$L_{xy} = 0.9\left(\frac{2\pi}{FWHM_{Qxy}}\right)$$

SUPPORTING FIGURES AND TABLES

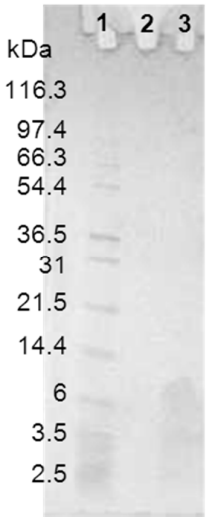

Supplemental Figure S1. Coomassie stained SDS-PAGE of purified deuterated RcLPS. Lane 1: molecular weight marker (in kDa), Lane 2: blank, Lane 3: deuterated RcLPS showing no protein contamination.

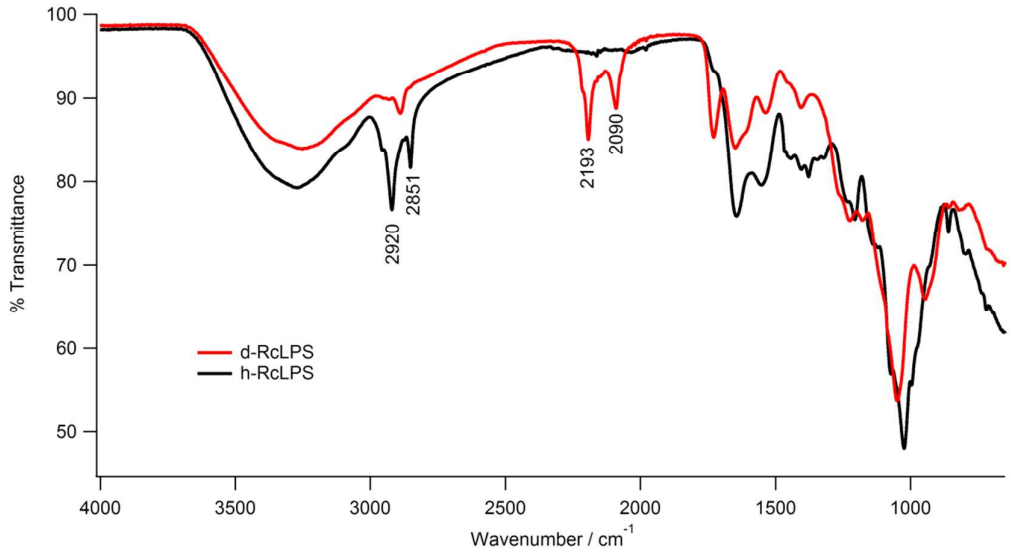

Supplementary Figure S2. FTIR spectra of hydrogenous RcLPS (black) and deuterated RcLPS (red) from *E. coli* J5. The peaks at 2193 and 2090 correspond to C-D bonds and the peaks at 2920 and 2851 correspond to C-H bonds.

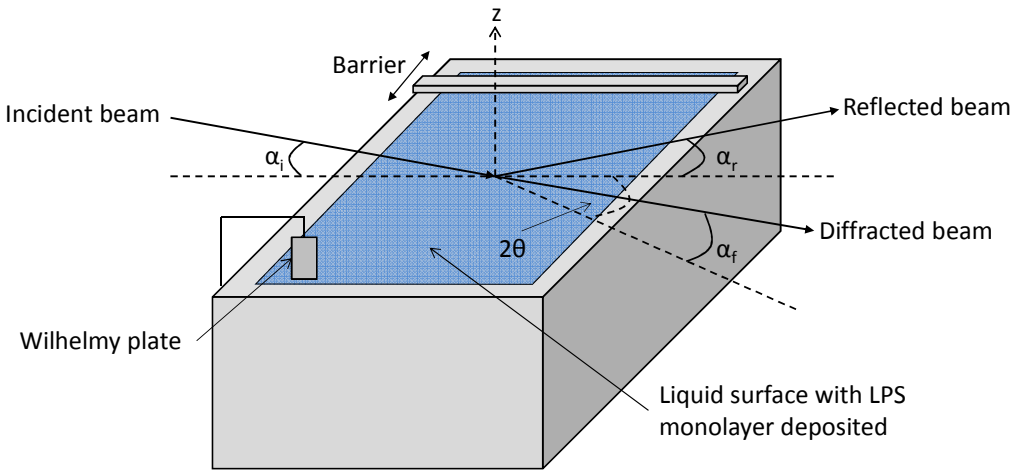

Supplemental Figure S3. Experimental set-up of the synchrotron XRR and GIXD. In the specular X-ray reflectivity mode the incident angle, α_i, equals the reflected angle, α_r, and the horizontal scattering angle, $2\theta = 0$ while in the grazing incidence X-ray diffraction mode α_i is fixed to 85 % of the critical angle, α_c, and $2\theta \neq 0$.

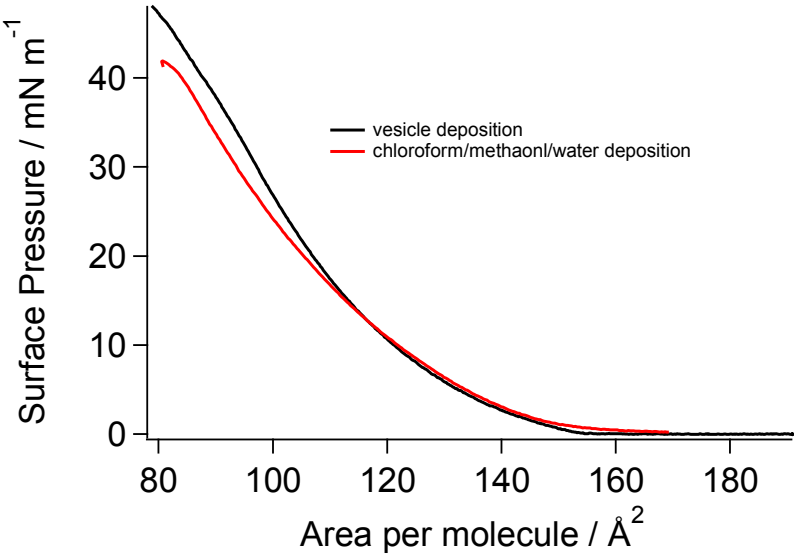

Supplementary Figure S4. Comparison of the area-pressure isotherms of a monolayer of RcLPS at the air-liquid interface by vesicle deposition (black trace) as described by Clifton *et al* (ref 10 in main text) or from spreading from chloroform/ methanol/water (6:4:1 by volume) (red trace).

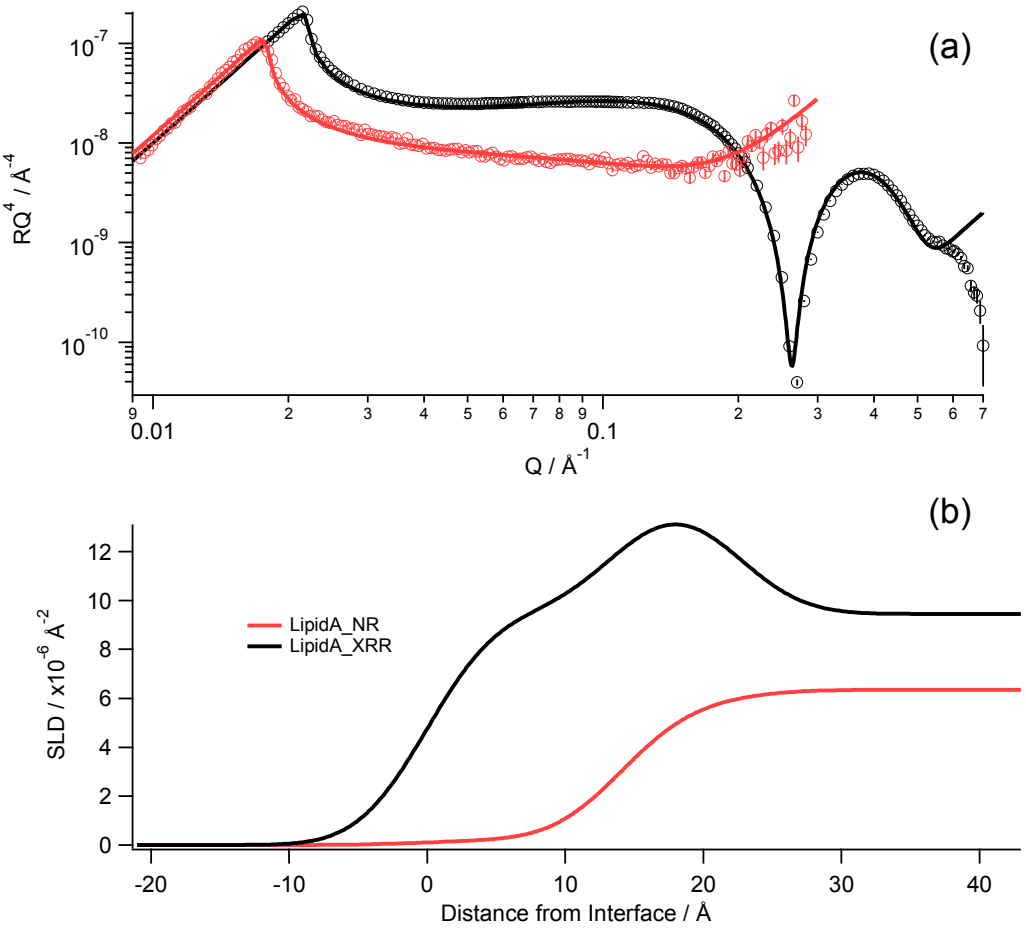

Supplementary Figure S5. a) The reflectivity data (symbols with error bars) and fits (solid lines) of lipid A at the air-water interface under pressure control at 20 mN m^{-1}. Two contrasts were fitted globally with h-lipid A on H_2O using X-rays (black) and h-lipid A on D_2O using neutrons (red). b) The corresponding real-space SLD profile of h-lipid A on H_2O measured using X-rays (black) and h-lipid A on D_2O measured using neutrons (red).

Supplementary Table S1. The theoretical neutron and X-ray scattering length density values of the different components of LPS.

Component	Formula[a]	Number of exchangeable protons / deuterons	nSLD in D_2O / $\times 10^{-6}$ Å^{-2}	nSLD in ACMW / $\times 10^{-6}$ Å^{-2}	xrSLD / $\times 10^{-6}$ Å^{-2}
h-myristic tails	$C_{13}H_{27}$	0	-0.37	-0.37	9.74
d-myristic tails	$C_{13}D_{27}$	0	6.82	6.82	9.74
h-lipid A HG[b]	$C_{24}H_{27}O_{22}N_2P_2$	8	3.39	2.58	18.2
d-lipid A HG	$C_{24}D_{27}O_{22}N_2P_2$	8	6.02	4.60	18.2
h-kdo[c]	$C_8H_{12}O_8$	6	4.04	2.10	16.7
d-kdo	$C_8D_{12}O_8$	6	6.20	4.95	16.7
h-heptose	$C_7H_{12}O_7$	6	4.48	2.07	18.3
d-heptose	$C_7D_{12}O_7$	6	7.15	5.61	18.3
h-hexose	$C_6H_{10}O_6$	5	4.54	2.16	18.6
d-hexose	$C_6D_{10}O_6$	5	7.18	5.66	18.6
h-hexosamine	$C_6H_{13}O_6N$	6	5.06	2.20	18.6
d-hexosamine	$C_6D_{13}O_6N$	6	7.70	6.18	18.6

[a] The volumes used to calculate SLD values are based around the crystal structures of sugars [11] and X-ray diffraction data for lipid tails.[12] [b] The lipid A head group consists of the phosphorylated N-acetylglucosamines and the carboxylic acid groups of the fatty acid chains. [c] kdo: 2-keto-3-deoxyoctonoic acid.

Supplementary Table S2. Results of globally fitting NR and XRR data of a lipid A monolayer at the air-liquid interface at 20 mN m^{-1}.

	Thickness / Å	xrSLD Lipid A / $\times 10^{-6}$ Å^{-2}	nSLD Lipid A on D_2O / $\times 10^{-6}$ Å^{-2}
Tails	14 ± 1	9.50 ± 0.09	0.21 ± 0.27
Headgroup	8 ± 1	14.70 ± 0.07	5.72 ± 0.52

SUPPORTING REFERENCES

(1) Chen, X.; Wilde, K. L.; Wang, H.; Lake, V.; Holden, P. J.; Middelberg, A. P. J.; He, L.; Duff, A. P. *Food Bioprod. Process.* **2012**, *90*, 563.

(2) Galanos, C.; Lüderitz, O.; Westphal, O. *Eur. J. Biochem.* **1969**, *9*, 245.

(3) Nelson, A. *J. Appl. Crystallogr.* **2006**, *39*, 273.

(4) Penfold, J. In *Neutron, X-ray and Light Scattering: Introduction to an Investigative Tool for Colloidal and Polymeric Systems* Lindner, P., Zemb, T., Eds.; Elsevier: Amsterdam, 1991, p 223.

(5) Holt, S. A.; Le Brun, A. P.; Majkrzak, C. F.; McGillivray, D. J.; Heinrich, F.; Loesche, M.; Lakey, J. H. *Soft Matter* **2009**, *5*, 2576.

(6) Heinrich, F.; Ng, T.; Vanderah, D. J.; Shekhar, P.; Mihailescu, M.; Nanda, H.; Losche, M. *Langmuir* **2009**, *25*, 4219.

(7) Kjaer, K. *Phys. B (Amsterdam, Neth.)* **1994**, *198*, 100.

(8) Jacquemain, D.; Wolf, S. G.; Leveiller, F.; Deutsch, M.; Kjaer, K.; Als-Nielsen, J.; Lahav, M.; Leiserowitz, L. *Angew. Chem., Int. Ed.* **1992**, *31*, 130.

(9) Jensen, T. R.; Kjaer, K. In *Novel Methods to Study Interfacial Layers*; Moebius, D., Miller, R., Eds.; Elsevier Science B. V.: Amsterdam, 2001, p 205.

(10) Kaganer, V. M.; Möhwald, H.; Dutta, P. *Rev. Mod. Phys.* **1999**, *71*, 779.

(11) Ferrier, W. G. *Acta Cryst.* **1960**, *13*, 678.

(12) Nagle, J. F.; Tristram-Nagle, S. *Biochim. Biophys. Acta, Rev. Biomembr.* **2000**, *1469*, 159.